

Nonlinear cross-Kerr quasiclassical dynamics

This content has been downloaded from IOPscience. Please scroll down to see the full text.

2013 New J. Phys. 15 043038

(<http://iopscience.iop.org/1367-2630/15/4/043038>)

View [the table of contents for this issue](#), or go to the [journal homepage](#) for more

Download details:

IP Address: 131.188.201.33

This content was downloaded on 06/02/2014 at 13:25

Please note that [terms and conditions apply](#).

Nonlinear cross-Kerr quasiclassical dynamics

I Rigas^{1,2}, A B Klimov³, L L Sánchez-Soto^{1,2,5} and G Leuchs^{1,4}

¹ Max-Planck-Institut für die Physik des Lichts, Günther-Scharowsky-Straße 1, Bau 24, D-91058 Erlangen, Germany

² Departamento de Óptica, Facultad de Física, Universidad Complutense, E-28040 Madrid, Spain

³ Departamento de Física, Universidad de Guadalajara, 44420 Guadalajara, Jalisco, Mexico

⁴ Department für Physik, Universität Erlangen-Nürnberg, Staudtstraße 7, D-91058 Erlangen, Germany

E-mail: lsanchez@fis.ucm.es

New Journal of Physics **15** (2013) 043038 (18pp)


Received 6 February 2013

Published 19 April 2013

Online at <http://www.njp.org/>

doi:10.1088/1367-2630/15/4/043038

Abstract. We study the quasiclassical dynamics of the cross-Kerr effect. In this approximation, the typical periodical revivals of the decorrelation between the two polarization modes disappear and remain entangled. By mapping the dynamics onto the Poincaré space, we find simple conditions for polarization squeezing. When dissipation is taken into account, the shape of the states in such a space is not considerably modified, but their size is reduced.

 Online supplementary data available from stacks.iop.org/NJP/15/043038/mmedia

⁵ Author to whom any correspondence should be addressed.



Content from this work may be used under the terms of the [Creative Commons Attribution 3.0 licence](http://creativecommons.org/licenses/by/3.0/). Any further distribution of this work must maintain attribution to the author(s) and the title of the work, journal citation and DOI.

Contents

1. Introduction	2
2. Cross-Kerr quasiclassical evolution	3
3. Mode correlation dynamics	5
4. Polarization squeezing	8
5. Mapping the dynamics on the sphere	10
6. Dissipative effects	11
7. Concluding remarks	14
Acknowledgments	14
Appendix A. The two-mode Wigner function	14
Appendix B. Purity of the reduced density matrix	15
References	16

1. Introduction

The optical Kerr effect refers to the intensity-dependent phase shift that a light field experiences during its propagation through a third-order nonlinear medium. This leads to a remarkable non-Gaussian operation that has sparked considerable interest due to potential applications in a variety of areas, such as quantum non-demolition measurements [1–9], generation of quantum superpositions [10–19], quantum teleportation [20–22], quantum logic [23–28] and single-particle detectors [29–31], to cite only a few.

Enhanced Kerr nonlinearities have been observed in electromagnetically induced transparency [32–35], Bose–Einstein condensates [36], cold atoms [37] and Josephson junctions [38–40]. Additional arrangements involve the Purcell effect [41], Rydberg atoms [42], light-induced Stark shifts [43] and nanomechanical resonators [44].

Special mention must be made of the role this cubic nonlinearity has played in the generation of squeezed light. The first proposals employed schemes involving a nonlinear interferometer [45] or degenerate four-wave mixing [46, 47]. But quite soon optical fibers became the paradigm for that purpose [48–53]. However, due to the typically small values of the nonlinearity in silica glass [54], Kerr-based fibers need long propagation distances and high powers, which bring other unwanted effects [55, 56].

In this paper, we direct our attention on this limit of high intensities, in which one could expect a classical description to be pertinent. Under reasonable assumptions, Maxwell's equations lead to a set of coupled nonlinear Schrödinger equations that has long been a useful tool for depicting the behavior of optical fields in nonlinear dispersive media. It has proved valuable in the description of such diverse phenomena as pulse compression, dark soliton formation and self-focusing of ultrashort pulses [57]. However, there remain non-classical features that cannot be explained in this classical manner. To put it differently, at the most basic level, the propagation of light in a Kerr medium is accompanied by unavoidable quantum effects.

The considerations so far indicate that the regime we wish to explore can be regarded as a problem at the boundary between classical and quantum worlds. Probably, the transition between both can be best scrutinized by exploiting phase-space methods [58–60]. This opens

up the possibility of gaining some information about the non-classical behavior with a quasiclassical description that employs essentially classical trajectories, while the correct quantum initial state is taken into account via, e.g., the Wigner function [61–63]. Despite some problems with the interpretation, the Wigner function has enjoyed substantial attention in various domains of physics [64] and has already been applied to some nonlinear problems in quantum optics [65–69].

The intensity dependence of the refractive index, which is the hallmark of the Kerr effect, can manifest itself in two different ways: as a self-phase modulation and as a cross-phase modulation. Self-phase modulation refers to the self-induced phase shift experienced by an optical field during its propagation, whereas cross-phase modulation refers to the nonlinear phase shift of an optical field induced by another one having a different wavelength, direction or state of polarization.

In this paper we focus on the cross-Kerr effect, for it is especially germane to attain polarization squeezing, a major goal in our laboratory [70]. We capitalize on the quasiclassical approach to re-analyze the light propagation in this case in a very concise way: after neglecting higher-order fluctuations, we obtain an evolution equation for the Wigner function that can be integrated to an analytical form. This allows us to study the dynamics of mode correlations. Since the resulting state is non-Gaussian, the application of common entanglement criteria [71, 72] becomes problematic, so we content ourselves with the study of the purity of the reduced states, which can be carried out in a closed form.

The two-mode Wigner function is appropriately cast in Poincaré space in terms of the phase-space version of the Stokes parameters, which affords an intuitive picture. Finally, as the Kerr dynamics is photon number preserving, the standard models of dissipation [73] based on coupling the modes to lossy reservoirs seem inadequate. Instead, we allow for dissipation through pure dephasing processes which turns out to be exactly solvable. The resulting evolution reveals that the shape of the Wigner functions is not considerably modified, but their size is shrunk.

2. Cross-Kerr quasiclassical evolution

As heralded in section 1, the cross-Kerr configuration corresponds to a situation in which the refractive index of a beam (say a) is modified by the intensity of a second one (say b). These beams are excited in two orthogonal polarization modes that, in a quantum description, are characterized by two complex amplitude operators, denoted as \hat{a} and \hat{b} , respectively. These operators obey the standard bosonic commutation relations

$$[\hat{a}, \hat{a}^\dagger] = \hat{1} = [\hat{b}, \hat{b}^\dagger], \quad [\hat{a}, \hat{b}] = 0 \quad (2.1)$$

the superscript \dagger standing for the adjoint.

In terms of these annihilation and creation operators, the Hamiltonian accounting for the cross-Kerr interaction is [74]

$$\hat{H} = \hbar\chi \hat{a}^\dagger \hat{a} \hat{b}^\dagger \hat{b}, \quad (2.2)$$

where χ is an effective coupling constant that depends on the third-order nonlinear susceptibility. For any state described by the density operator $\hat{\rho}$, the evolution is given by

$$i\hbar\partial_t \hat{\rho} = [\hat{H}, \hat{\rho}], \quad (2.3)$$

whose solution can be formally written as

$$\hat{\rho}(t) = \exp(-i t \hat{H}/\hbar) \hat{\rho}(0) \exp(i t \hat{H}/\hbar). \quad (2.4)$$

By expanding this equation in the two-mode Fock basis $|n_a, n_b\rangle$, the evolution may be, in principle, tracked. Take the example of an initially pure, two-mode coherent state $|\Psi(0)\rangle = |\alpha_0, \beta_0\rangle$, where henceforth the subscript 0 indicates the value of the corresponding variable at $t = 0$. The resulting state is

$$\begin{aligned} |\Psi(t)\rangle &= \exp(-i t \hat{H}/\hbar) |\Psi(0)\rangle \\ &= \exp[-(|\alpha_0|^2 + |\beta_0|^2)/2] \sum_{n_a, n_b=0}^{\infty} \frac{\alpha_0^{n_a} \beta_0^{n_b}}{\sqrt{n_a! n_b!}} \exp(-i \chi t n_a n_b) |n_a, n_b\rangle. \end{aligned} \quad (2.5)$$

The term $\exp(-i \chi t n_a n_b)$ arises because of the coupling between the modes and causes that the state cannot be factorized into single-mode states; that is, it becomes entangled, as we shall examine in the next section.

It is apparent that equation (2.5) is of practical use only for few-photon states. Actually, such an exact solution does not allow us to extract the classical part of the dynamics in a manifest form. To that end, we proceed to decompose the mode operators \hat{a} and \hat{b} as

$$\hat{a} = \alpha + \delta\hat{a}, \quad \hat{b} = \beta + \delta\hat{b}, \quad (2.6)$$

that is, a sum of classical amplitudes and quantum noise operators. The average values of the noise operators are assumed to be much smaller than the corresponding coherent amplitudes ($|\alpha|^2, |\beta|^2 \gg 1$), so we can restrict the analysis to first-order terms in $\delta\hat{a}$ and $\delta\hat{b}$. If we employ the two-mode Wigner function $W(\alpha, \beta)$ and the basic techniques outlined in appendix A, equation (2.4), with this linearization ansatz, can be recast as

$$i \partial_t W = \chi |\beta|^2 \left(\alpha^* \frac{\partial W}{\partial \alpha^*} - \alpha \frac{\partial W}{\partial \alpha} \right) + \chi |\alpha|^2 \left(\beta^* \frac{\partial W}{\partial \beta^*} - \beta \frac{\partial W}{\partial \beta} \right). \quad (2.7)$$

Two comments are in order here. Firstly, we are ignoring quantum fluctuations, inasmuch as we are disregarding higher-order moments of the noise operators; this seems a plausible approximation for highly excited fields. Secondly, we underline that the evolution is specified only by classical trajectories, much in the spirit of the quasiclassical approximation.

To shed light on the physics embodied in (2.7), we resort to action-angle variables (\mathcal{I}, φ) for each mode [75]. In our context, they can be defined as

$$\alpha = \sqrt{\mathcal{I}_a} \exp(i \varphi_a), \quad \beta = \sqrt{\mathcal{I}_b} \exp(i \varphi_b), \quad (2.8)$$

and therefore φ is the polar angle in phase space, whereas \mathcal{I} is related to the mode intensity (see figure 1). With these variables, equation (2.7) can be rewritten in a simple and elegant form

$$\partial_t W = \chi \mathcal{I}_b \frac{\partial W}{\partial \varphi_a} + \chi \mathcal{I}_a \frac{\partial W}{\partial \varphi_b}. \quad (2.9)$$

As $\partial/\partial\varphi$ generates rotations in phase space, equation (2.9) reflects that the amplitudes in each mode experience different rotations, with angles proportional to the intensity components of the other mode [76, 77]. The result is schematized in figure 1: roughly speaking, the shaded area indicates the region in phase space occupied by the state. For an initial coherent state this area is a circle; the top of the circle corresponds to higher intensity and therefore is more phase shifted than the bottom, resulting in an elliptical noise distribution.

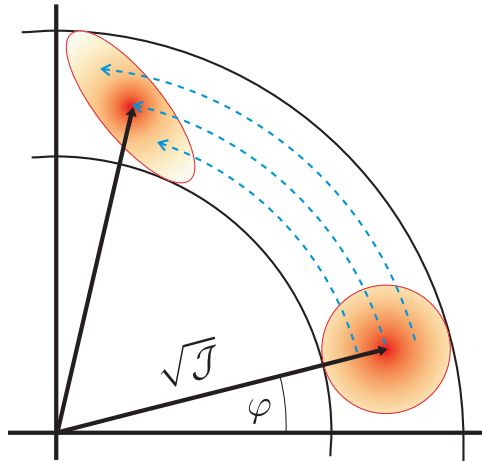


Figure 1. Schematic representation, in the phase space of a single mode, of the effect of a Kerr medium. The initial state is a coherent state, represented by a circle noise determined by the uncertainty relation. It experiences a rotation of angle depending on the different amplitudes $\sqrt{\mathcal{I}}$. The final result is an elliptical noise distribution.

Equation (2.9) can be readily solved:

$$W(\mathcal{I}_a, \varphi_a; \mathcal{I}_b, \varphi_b | t) = W(\mathcal{I}_a, \varphi_a + \mathcal{I}_b \chi t; \mathcal{I}_b, \varphi_b + \mathcal{I}_a \chi t | 0). \quad (2.10)$$

If again we assume initially the two-mode coherent state $|\alpha_0, \beta_0\rangle$ ($\alpha_0 = \sqrt{\mathcal{I}_{0a}} e^{i\varphi_{0a}}$, $\beta_0 = \sqrt{\mathcal{I}_{0b}} e^{i\varphi_{0b}}$), then using (A.5), equation (2.10) reduces to

$$W(\mathcal{I}_a, \varphi_a; \mathcal{I}_b, \varphi_b | \tau) = \frac{4}{\pi^2} \exp \left[-2 \left| \sqrt{\mathcal{I}_a} e^{i(\varphi_a + 2\mathcal{I}_b \tau)} - \sqrt{\mathcal{I}_{0a}} e^{i\varphi_{0a}} \right|^2 \right] \\ \times \exp \left[-2 \left| \sqrt{\mathcal{I}_b} e^{i(\varphi_b + 2\mathcal{I}_a \tau)} - \sqrt{\mathcal{I}_{0b}} e^{i\varphi_{0b}} \right|^2 \right], \quad (2.11)$$

where we have introduced the dimensionless variable $\tau = \chi t/2$. Observe that at $\tau = 0$ the Wigner function is made of two independent Gaussians, while as time goes by the induced mode correlations lead to a non-Gaussian state.

3. Mode correlation dynamics

Two-mode Gaussian states constitute the simplest example of a continuous-variable bipartite system, the workhorses of quantum information. Accordingly, the theoretical aspects of these states have been extensively worked out and a variety of quantitative characterizations are available for them [78–82].

A unique feature of these Gaussian states is that they are fully specified (up to local displacements) by the covariance matrix $\boldsymbol{\gamma}$, with elements $\gamma_{ij} = \text{Tr}[\hat{\rho}\{\hat{R}_i, \hat{R}_j\}/2]$, where $\{, \}$ denotes the anticommutator and $\hat{\mathbf{R}} = (\hat{x}_a, \hat{p}_a, \hat{x}_b, \hat{p}_b)$ is the vector of phase-space operators. This covariance matrix can be jotted down as

$$\boldsymbol{\gamma} = \begin{pmatrix} \mathbf{A} & \mathbf{C} \\ \mathbf{C}^t & \mathbf{B} \end{pmatrix}. \quad (3.1)$$

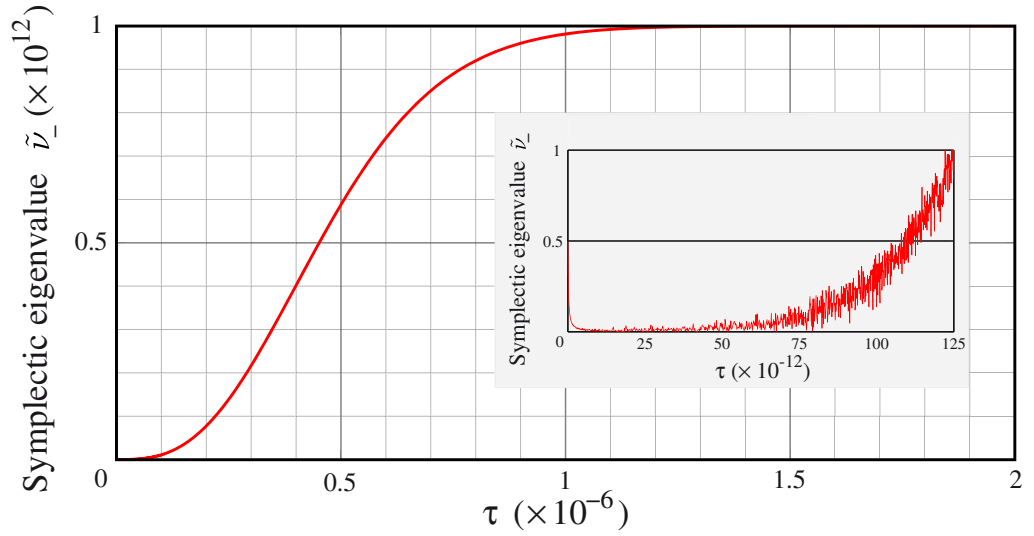


Figure 2. Time evolution of the symplectic eigenvalue $\tilde{\nu}_-$ of the state (2.11), as a measure of the entanglement between the two modes. We have taken both modes with the same intensity $\mathcal{I}_{0a} = \mathcal{I}_{0b} = 10^6$. Entanglement is proven for $\tilde{\nu}_- < 0.5$, a region that can be observed only in the inset.

Here, \mathbf{A} and \mathbf{B} are the covariance matrices associated with the reduced state of the modes a and b , while \mathbf{C} describes the correlation between these modes. The symplectic eigenvalues of $\boldsymbol{\gamma}$ are

$$\nu_{\pm}^2 = \frac{1}{2} \left[\Delta \pm \sqrt{\Delta^2 - 4 \det \boldsymbol{\gamma}} \right] \quad (3.2)$$

with $\Delta = \det \mathbf{A} + \det \mathbf{B} + 2 \det \mathbf{C}$. These symplectic eigenvalues encode all the essential information and provide powerful, simple ways for to express fundamental properties. For example, a Gaussian state is entangled if and only if

$$\tilde{\nu}_- < 1/2, \quad (3.3)$$

where the smallest symplectic eigenvalue $\tilde{\nu}_-$ of the covariance matrix corresponding to the partially transposed state is obtained from ν_- by replacing $\det \mathbf{C}$ with $-\det \mathbf{C}$, i.e. by time reversal in the second system and thus a flip of its canonical momentum.

In figure 2 we have plotted the time evolution of $\tilde{\nu}_-$ for the state (2.11), showing a rapid increase (in the inset, we observe a fluctuating behavior that is smeared out in a larger scale). The main caveat with this approach is that, as mentioned before, our state rapidly becomes non-Gaussian, and criterion (3.3) gives then only a sufficient condition. Consequently, we can certify entanglement just in the short-time window displayed in the inset. This actually holds for any available criterion [71, 72]: if the state is entangled, a given test may or may not detect its entanglement; in turn, if a particular test does not detect entanglement, we cannot conclude separability of the state.

Genuine non-Gaussian entanglement can only be revealed by measures involving higher-order moments. In this vein, Shchukin and Vogel [83] (see also [84, 85]) have introduced a general hierarchy of necessary and sufficient conditions for any state to be entangled. Nevertheless, the application of this technique to our problem turns out to be very arduous for it

involves checking non-trivial inequalities, which can be performed only numerically. Moreover, the method involves the determination of moments that are extremely oscillatory and noisy [86].

In view of these difficulties, we content ourselves with assessing the purity of the reduced state of both modes. This is related to the linear entropy and is intimately connected to the intermodal correlations [87]. These local purities are

$$P_a(\tau) = \text{Tr}_a[\hat{\rho}_a^2(\tau)], \quad P_b(\tau) = \text{Tr}_b[\hat{\rho}_b^2(\tau)], \quad (3.4)$$

$\hat{\rho}_a(\tau) = \text{Tr}_b[\hat{\rho}(\tau)]$ and $\hat{\rho}_b(\tau) = \text{Tr}_a[\hat{\rho}(\tau)]$ being the reduced density matrices of modes a and b , respectively. If we employ now the two-mode Wigner function (2.11), the purity, say $P_a(\tau)$, can be written as

$$P_a(\tau) = \frac{\pi}{8} \int_{-\pi}^{\pi} d\varphi_a \int_0^{\infty} d\mathcal{J}_a \left[\int_{-\pi}^{\pi} d\varphi_b \int_0^{\infty} d\mathcal{J}_b W(\mathcal{J}_a, \varphi_a; \mathcal{J}_b, \varphi_b | \tau) \right]^2. \quad (3.5)$$

For a bipartite system, both purities in (3.4) coincide for pure states [88, 89]. In general, these quantities are different for mixed states. In our case, after a long but otherwise straightforward calculation (which, for completeness, is sketched in appendix B), $P_a(\tau)$ can be displayed as

$$P_a(\tau) = \exp(-4\mathcal{J}_{0b} - 2\mathcal{J}_{0a}) \sum_{n=-\infty}^{\infty} \frac{I_n(2\mathcal{J}_{0a})}{1 + \tau^2 n^2} \exp\left(\frac{4\mathcal{J}_{0b}}{1 + \tau^2 n^2}\right) = P_b(\tau), \quad (3.6)$$

where $I_n(z)$ are the modified Bessel functions of the first kind and the last equality has been carefully checked by numerical experiments. This surprising symmetry can be ascribed to the way in which the modes enter the Kerr Hamiltonian (2.2). Accordingly, we drop the mode subscripts in the purities.

As we are dealing with highly excited fields ($\mathcal{J}_{0a} \gg 1$), we can make use of the asymptotic expansion [90]

$$I_n(z) \sim \frac{e^z}{\sqrt{2\pi z}} e^{-n^2/2z}, \quad |z| \gg 1. \quad (3.7)$$

In addition, as $\tau \ll 1$ and the functions in (3.6) do not oscillate, we can replace the summation by an integral, the final result being

$$P(\tau) = \frac{1}{\sqrt{4\pi \mathcal{J}_{0a}}} \int_{-\infty}^{\infty} dx \frac{1}{1 + \tau^2 x^2} \exp\left(-\frac{4\mathcal{J}_{0b}\tau^2 x^2}{1 + \tau^2 x^2} - \frac{x^2}{4\mathcal{J}_{0a}}\right). \quad (3.8)$$

In figure 3, we plot the time evolution of this $P(\tau)$ in the same scale as in figure 2. At $\tau = 0$ the reduced purity is unity, in agreement with the fact that initially the state consists of two uncorrelated Gaussians. As time evolves, the purity smoothly decreases (much in the same way as the symplectic eigenvalue $\tilde{\nu}_-$ decreases), which indicates the presence of mode correlations. This is supported by the following asymptotic estimate of (3.8):

$$P(\tau) \simeq \frac{1}{\sqrt{1 + 16\mathcal{J}_{0a}\mathcal{J}_{0b}\tau^2}} \quad (3.9)$$

valid for $\mathcal{J}_{0b}\tau \lesssim 1$. It is clear that this form of $P(\tau)$ is invariant under mode permutations. Finally, $P(\tau)$ tends to its stationary value.

One might wonder how quantum fluctuations, neglected so far, could modify this quasiclassical picture. For the particular case of initial coherent states we are treating here,

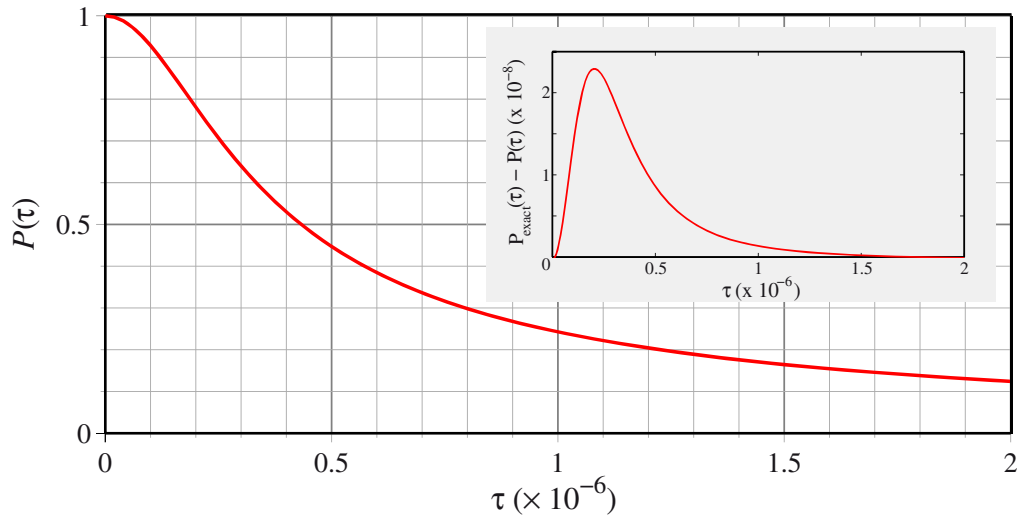


Figure 3. Evolution of the purity $P(\tau)$ as a measure of the correlations between the two modes for the same conditions as in figure 2.

we can analytically compute the purity for the exact quantum solution. Indeed, from (2.5) we have

$$\hat{\rho}_a(t) = \exp[-|\alpha_0|^2 - |\beta_0|^2] \sum_{n_a, n_b=0}^{\infty} \frac{\alpha_0^{n_a} \alpha_0^{*n_b}}{\sqrt{n_a! n_b!}} \exp[e^{2i\tau(n_a - n_b)} |\beta_0|^2] |n_a\rangle \langle n_b|, \quad (3.10)$$

wherefrom one can easily derive the exact expression for the purity:

$$P_{\text{exact}}(\tau) = \exp(-2\mathcal{J}_{0a} - 2\mathcal{J}_{0b}) \sum_{n=-\infty}^{\infty} I_n(2\mathcal{J}_{0b}) \exp[2\mathcal{J}_{0a} \cos(2n\tau)]. \quad (3.11)$$

Using the properties of the Bessel functions, we redraft this as

$$P_{\text{exact}}(\tau) = \exp(-2\mathcal{J}_{0a} - 2\mathcal{J}_{0b}) \sum_{m, n=-\infty}^{\infty} I_m(2\mathcal{J}_{0a}) I_n(2\mathcal{J}_{0b}) \exp(2imn\tau), \quad (3.12)$$

which explicitly exhibits the aforementioned symmetry. In fact, taking into account (3.7), $P_{\text{exact}}(\tau)$ appears as a bidimensional Jacobi theta function [90], which is periodic. However, in the time scales we are considering here, such a periodicity is unnoticeable and we can replace again the sum by an integral, getting precisely equation (3.9).

In the inset of figure 3, we have plotted the difference between the exact solution (3.12) and the quasiclassical one (3.8). As we can see, both solutions coincide for any practical purpose. This means that the correlations examined before are of quantum nature, but higher-order correlations play no relevant role here.

4. Polarization squeezing

Since the polarization modes a and b have the same frequency and are orthogonal, their superposition results in a general elliptical polarization. This means that one needs only three

independent quantities: the amplitudes of each mode and the relative phase between them. To describe this at the quantum level, it is advantageous to use the Stokes operators [91]

$$\hat{S}_x = \hat{a}^\dagger \hat{b} + \hat{b}^\dagger \hat{a}, \quad \hat{S}_y = i(\hat{a} \hat{b}^\dagger - \hat{a}^\dagger \hat{b}), \quad \hat{S}_z = \hat{a}^\dagger \hat{a} - \hat{b}^\dagger \hat{b} \quad (4.1)$$

complemented with the total number $\hat{N} = \hat{a}^\dagger \hat{a} + \hat{b}^\dagger \hat{b}$. On account of (2.1), the operators (4.1) satisfy the commutation relations of an angular momentum

$$[\hat{S}_k, \hat{S}_\ell] = 2i \varepsilon_{k\ell m} \hat{S}_m, \quad [\hat{N}, \hat{S}_k] = 0, \quad (4.2)$$

where the Latin indices run over $\{x, y, z\}$ and $\varepsilon_{k\ell m}$ is the Levi–Civita fully antisymmetric tensor. This non-commutability precludes the simultaneous exact measurement of the physical quantities they represent and leads immediately to the Heisenberg inequalities [92–95]

$$\Delta^2 \hat{S}_k \Delta^2 \hat{S}_\ell \geq \varepsilon_{k\ell m} |\langle \hat{S}_m \rangle|^2, \quad (4.3)$$

where $\Delta^2 \hat{A} = \langle \hat{A}^2 \rangle - \langle \hat{A} \rangle^2$ indicates the variance. It is always possible to find pairs of maximally conjugate operators for this uncertainty relation. This is equivalent to establishing a basis in which only one of the operators (4.1) has a non-zero expectation value, say $\langle \hat{S}_k \rangle = \langle \hat{S}_\ell \rangle = 0$ and $\langle \hat{S}_m \rangle \neq 0$. The only non-trivial Heisenberg inequality reads thus

$$\Delta^2 \hat{S}_k \Delta^2 \hat{S}_\ell \geq |\langle \hat{S}_m \rangle|^2. \quad (4.4)$$

Polarization squeezing can then be sensibly defined by the condition [96–100]

$$\Delta^2 \hat{S}_k < |\langle \hat{S}_m \rangle| < \Delta^2 \hat{S}_\ell. \quad (4.5)$$

Note that squeezed states according to (4.5) are not, in general, minimum uncertainty states.

The choice of the conjugate operators $\{\hat{S}_k, \hat{S}_\ell\}$ is by no means unique: there exists an infinite set $\{\hat{S}_\perp(\vartheta), \hat{S}_\perp(\vartheta + \pi/2)\}$ that are perpendicular to the classical excitation $\langle \hat{S}_m \rangle$, for which $\langle \hat{S}_\perp(\vartheta) \rangle = 0$ for all ϑ . All these pairs exist in the S_k – S_ℓ plane, which is called the *dark plane*. A generic $\hat{S}_\perp(\vartheta)$ can be written as

$$\hat{S}_\perp(\vartheta) = \hat{S}_k \cos \vartheta + \hat{S}_\ell \sin \vartheta, \quad (4.6)$$

ϑ being an angle defined relative to \hat{S}_k . Condition (4.5) is then equivalent to

$$\Delta^2 \hat{S}_\perp(\vartheta_{\text{sq}}) < |\langle \hat{N} \rangle| < \Delta^2 \hat{S}_\perp(\vartheta_{\text{sq}} + \pi/2), \quad (4.7)$$

where $\hat{S}_\perp(\theta_{\text{sq}})$ is the maximally squeezed operator and $\hat{S}_\perp(\theta_{\text{sq}} + \pi/2)$ the antisqueezed one.

In many experiments both modes have the same amplitude but are phase shifted by $\pi/2$: $\langle \hat{a} \rangle = i \langle \hat{b} \rangle$. This light is circularly polarized and fulfills $\langle \hat{S}_x \rangle = \langle \hat{S}_z \rangle = 0$, $\langle \hat{S}_y \rangle \neq 0$, so (4.7) directly applies.

The time evolution of the variables involved in those definitions can be evaluated using the Wigner-distribution approach:

$$\langle \hat{S}_\perp(\vartheta, \tau) \rangle = \pi^2 \text{Re} \left[e^{i\vartheta} \int d^2\alpha d^2\beta W_{\hat{S}_\perp(\vartheta)}(\alpha, \beta) W(\alpha, \beta|\tau) \right]. \quad (4.8)$$

Here, $W_{\hat{S}_\perp(\vartheta)}(\alpha, \beta)$ refers to the phase-space function corresponding to the operator $\hat{S}_\perp(\vartheta)$ (commonly called its symbol). From (4.1) and (4.6) it is clear that the symbol of $\hat{S}_\perp(\vartheta)$ can be directly constructed in terms of the symbols of the basic mode amplitudes \hat{a} and \hat{b} , which,

from appendix A, we know are given by $W_{\hat{a}}(\alpha) = \alpha/\pi$ and $W_{\hat{b}}(\beta) = \beta/\pi$. Therefore, we obtain

$$\langle \hat{S}_y(\tau) \rangle = \frac{\mathcal{I}_0}{(1+\tau^2)^2} \exp\left(-\frac{2\mathcal{I}_0\tau^2}{1+\tau^2}\right), \quad \langle \hat{S}_x(\tau) \rangle = \langle \hat{S}_z(\tau) \rangle = 0, \quad (4.9)$$

where $\mathcal{I}_0 = \text{Tr}[\hat{\rho}(0)\hat{N}]$ is the initial average number of photons of the state. The second-order moments are calculated much in the same way; the final result is

$$\begin{aligned} \Delta^2 \hat{S}_{\perp}(\vartheta, \tau) = & \mathcal{I}_0[1 + (\mathcal{I}_0/2) \sin^2 \vartheta] - \sin^2(\vartheta/2) \frac{2\mathcal{I}_0^2}{(1+4\tau^2)^3} \exp\left(-\frac{8\mathcal{I}_0\tau^2}{1+4\tau^2}\right) \\ & - \sin(2\vartheta) \frac{2\mathcal{I}_0\tau}{(1+\tau^2)^3} \left(1 + \frac{\mathcal{I}_0}{1+\tau^2}\right) \exp\left(-\frac{2\mathcal{I}_0\tau^2}{1+\tau^2}\right). \end{aligned} \quad (4.10)$$

A major advantage of this formalism is that we can specify the time evolution of polarization squeezing. In particular, for sufficiently short times $\tau \ll 1$, we can expand equations (4.9) and (4.10) up to second order, so that

$$\langle \hat{S}_y(\tau) \rangle \simeq \mathcal{I}_0(1 - \mathcal{I}_0\tau^2), \quad \Delta^2 \hat{S}_{\perp}(\vartheta, \tau) \simeq \mathcal{I}_0[1 + 4\mathcal{I}_0^2 \sin^2(\vartheta) \tau^2] - 2\mathcal{I}_0^2 \sin(2\vartheta)\tau, \quad (4.11)$$

so that the optimal squeezing angle is roughly given by

$$\vartheta_{\text{sq}} \simeq \frac{1}{2} \text{arccot}(\mathcal{I}_0\tau), \quad (4.12)$$

i.e. it starts at $\vartheta_{\text{sq}} = \pi/4$ and slowly moves toward 0 as τ goes by.

5. Mapping the dynamics on the sphere

It is possible to turn the action of the Stokes operators discussed in the previous section into a very simple phase-space picture. To this end we introduce the parametrization [101]

$$\alpha = \sqrt{\mathcal{I}} e^{i\varphi_a} \cos(\theta/2), \quad \beta = \sqrt{\mathcal{I}} e^{i\varphi_a} e^{-i\phi} \sin(\theta/2), \quad (5.1)$$

where φ_a appears now as a global phase and the pertinent relative phase is $\phi = \varphi_a - \varphi_b$. The radial variable

$$\mathcal{I} = \mathcal{I}_a + \mathcal{I}_b \quad (5.2)$$

represents the total intensity. The parameters θ and ϕ can be interpreted as the polar and azimuthal angles, respectively, on the Poincaré sphere: θ describes the relative amount of intensity carried by each mode and ϕ is the relative phase between them. In terms of these new variables, equation (2.9) becomes

$$\partial_t W = \chi \mathcal{I}_b \frac{\partial W}{\partial \varphi_a} + \chi (\mathcal{I}_b - \mathcal{I}_a) \frac{\partial W}{\partial \phi}. \quad (5.3)$$

In (5.1), φ_a appears as an irrelevant global phase over which we can integrate without losing relevant information; the result is

$$\partial_t W(\mathcal{I}, \theta, \phi) = -\chi \mathcal{I} \cos \theta \frac{\partial W(\mathcal{I}, \theta, \phi)}{\partial \phi}, \quad (5.4)$$

whose solution in terms of the adimensional variable τ reads

$$W(\mathcal{I}, \theta, \phi|\tau) = W(\mathcal{I}, \theta, \phi - 2\tau \mathcal{I} \cos \theta|0). \quad (5.5)$$

The three numbers $(\mathcal{J}, \theta, \phi)$ are the spherical coordinates in the Poincaré space:

$$S_x = \mathcal{J} \sin \theta \cos \phi, \quad S_y = \mathcal{J} \sin \theta \sin \phi, \quad S_z = \mathcal{J} \cos \theta. \quad (5.6)$$

In terms of the Cartesian counterpart, equation (5.5) can be compactly expressed as

$$W(S_x, S_y, S_z|\tau) = \frac{8}{\pi} \exp(-2\mathcal{J} - 2\mathcal{J}_0) I_0 \left(2\sqrt{\sigma(\theta, \phi, \tau)} \right), \quad (5.7)$$

where

$$\sigma(\theta, \phi, \tau) = 2 \left[\mathcal{J} \mathcal{J}_0 + S_z S_{0z} + \cos(2S_z \tau) (S_x S_{0x} + S_y S_{0y}) + \sin(2S_z \tau) (S_y S_{0x} - S_x S_{0y}) \right]. \quad (5.8)$$

For the aforementioned case of circularly polarized light, with $S_{0x} = S_{0z} = 0$, $S_{0y} = \mathcal{J}_0$, this reduces to

$$\sigma(\theta, \phi, \tau) = 2\mathcal{J}_0 \left[\mathcal{J} + S_y \cos(2S_z \tau) - S_x \sin(2S_z \tau) \right]. \quad (5.9)$$

In the x - p quadrature phase space, the usual way of representing states is by an uncertainty region which is just a contour of the Wigner function $W(x, p)$ for that state. Much in the same way, for each fixed time, the equation $W(S_x, S_y, S_z|\tau) = \text{constant}$ defines an isocontour surface in the Poincaré space of the axes (S_x, S_y, S_z) , which gives complete information about the fluctuations of the state. In the supplementary material of this paper (available from stacks.iop.org/NJP/15/043038/mmedia), we include a movie portraying the time evolution of the Wigner function (5.7) for the particular instance in (5.9). As can be appreciated, the state gets elongated along the direction of maximal squeezing. In figure 4, we present three snapshots of the movie, corresponding to different times.

6. Dissipative effects

As light propagates through the Kerr medium, it experiences a decorrelation of the relative phase between both basic polarization modes. A sensible approach to deal with this decorrelation is through the notion of decoherence, by which we loosely understand the appearance of irreversible and uncontrollable quantum correlations when a system interacts with its environment [102].

Usually, decoherence is accompanied by dissipation, i.e. a net exchange of energy with the environment. However, given the nature of the Kerr nonlinearity, we are interested in the case of pure decoherence (also known as dephasing), for which the processes of energy dissipation are negligible. Models in which the number of photons do not change, while the coherences are strongly decaying, are at hand [103–107]. Surprisingly enough, however, they have not been applied in the context of the phase-number preserving Kerr dynamics. In consequence, we model such a dephasing by the master equation

$$\partial_t \hat{\rho} = -i[\hat{H}, \hat{\rho}] + \gamma_a \mathcal{L}_a[\hat{\rho}] + \gamma_b \mathcal{L}_b[\hat{\rho}], \quad (6.1)$$

where $\mathcal{L}_a[\hat{\rho}]$ is the Linblad superoperator

$$\mathcal{L}_a[\hat{\rho}] = 2\hat{a}^\dagger \hat{a} \hat{\rho} \hat{a}^\dagger \hat{a} - (\hat{a}^\dagger \hat{a})^2 \hat{\rho} - \hat{\rho} (\hat{a}^\dagger \hat{a})^2 \quad (6.2)$$

with γ_a the dephasing constant. A similar expression holds for mode b . The equation for the Wigner function (2.9) is modified now to

$$\partial_t W = \chi \mathcal{J}_b \frac{\partial W}{\partial \varphi_a} + \chi \mathcal{J}_a \frac{\partial W}{\partial \varphi_b} + \frac{\gamma_a}{4} \frac{\partial^2 W}{\partial \varphi_a^2} + \frac{\gamma_b}{4} \frac{\partial^2 W}{\partial \varphi_b^2}. \quad (6.3)$$

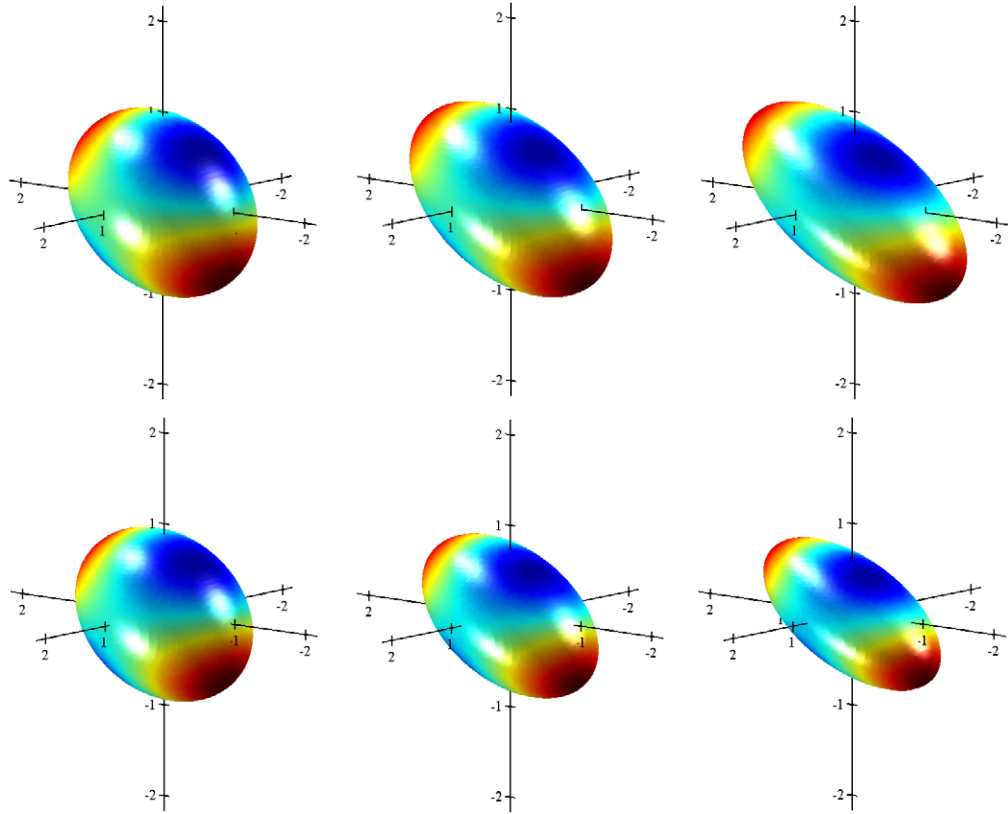


Figure 4. Isocontour surfaces of the level 10^{-4} (from the maximum) of the Wigner function $W(S_x, S_y, S_z|\tau) = \text{constant}$ at times $\tau = 1.5 \times 10^{-7}$, 3.0×10^{-7} and 4.5×10^{-7} (from left to right), without dephasing (top) and with a dephasing of $\gamma = 0.5\chi$ (bottom). The orthogonal axes are S_x , S_y and S_z , the box is centered at $S_x = S_z = 0$, $S_y = 10^6$ and the axis ticks are measured in units of the (spherical) isocontour at $\tau = 0$, which corresponds to the shot-noise limit.

Using again the variables (5.6) and integrating over the irrelevant overall phase φ_a , this equation turns out to be

$$\partial_t W(\mathcal{I}, \theta, \phi) = -\chi \mathcal{I} \cos \theta \frac{\partial W(\mathcal{I}, \theta, \phi)}{\partial \phi} + \frac{\gamma}{4} \frac{\partial^2 W(\mathcal{I}, \theta, \phi)}{\partial \phi^2} \quad (6.4)$$

with $\gamma = \gamma_a + \gamma_b$. Its general solution can be represented by

$$W(\mathcal{I}, \theta, \phi|t) = \frac{1}{2\pi} \int d\phi' \Theta(\phi - \phi' - \chi t \mathcal{I} \cos \theta | t \gamma / 4) W(\mathcal{I}, \theta, \phi'|0) \quad (6.5)$$

with $\Theta(\phi|t) = \sum_k \exp(ik\phi - tk^2)$. In the limit $\mathcal{I}_0 \gg 1$, this exact result simplifies to

$$W(\mathcal{I}, \theta, \phi|t) = \frac{2 \exp(-2\mathcal{I} - 2\mathcal{I}_0 + 4\mathcal{I}\mathcal{I}_0)}{\pi^2 \sqrt{\mathcal{I}\mathcal{I}_0} \sin \theta \sin \theta_0} \Theta\left(\phi - \phi_0 - \chi t \mathcal{I} \cos \theta \left| \frac{\gamma t}{4} + \frac{\cos[(\theta - \theta_0)/2]}{2S\mathcal{I}_0 \sin \theta \sin \theta_0} \right.\right). \quad (6.6)$$

The snapshots of the evolution of this Wigner function can be again appreciated in figure 4, with $\gamma = 2\gamma_a = 2\gamma_b = 0.5\chi$. While at the beginning one can only observe a very gentle difference with the non-dissipative case, this difference gets more visible as time goes by.

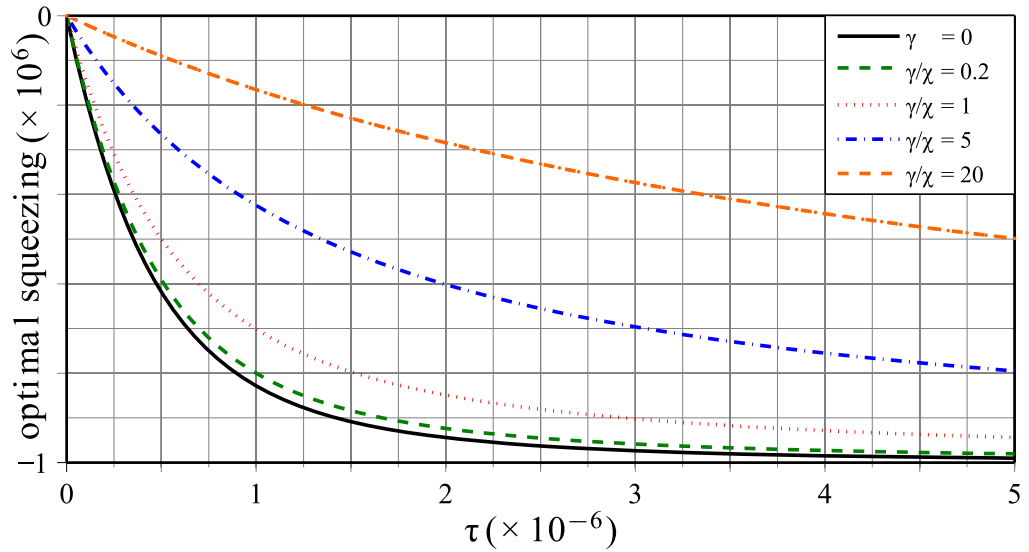


Figure 5. Optimal amount of squeezing $\Delta^2 \hat{S}_y^{\text{opt}}(t) - |\langle \hat{S}_y(t) \rangle|$. The values for γ/χ are 0 (black solid), 0.2 (green dashed), 1 (red dotted), 5 (blue dash-dotted) and 20 (orange dashed).

The shrinking of the isolevels of the Wigner function for the dissipative evolution means that it gets ‘smeared out’ over the phase space due to the dephasing. Note that the shape and the direction of the ellipsoids are not changed; only their size is different, indicating a lower degree of polarization.

We can also investigate the impact of dephasing on squeezing. To this end we need to calculate the corresponding quantities as in equations (4.9) and (4.10). One finally gets

$$\langle \hat{S}_y(t) \rangle = \frac{\mathcal{I}_0}{(1+\tau^2)^2} \exp\left(-\frac{2\mathcal{I}_0\tau^2}{1+\tau^2} - \frac{\gamma t}{4}\right) \quad (6.7)$$

$$\begin{aligned} \Delta^2 \hat{S}_\perp(\theta, t) = & \mathcal{I}_0[1 + (\mathcal{I}_0/2) \sin^2 \vartheta] - \sin^2(\vartheta/2) \frac{\mathcal{I}_0^2}{(1+4\tau^2)^3} \exp\left(-\frac{8\mathcal{I}_0\tau^2}{1+4\tau^2} - \gamma t\right) \\ & - \sin(2\vartheta) \frac{2\mathcal{I}_0\tau}{(1+\tau^2)^3} \left(1 + \frac{\mathcal{I}_0}{1+\tau^2}\right) \exp\left(-\frac{2\mathcal{I}_0\tau^2}{1+\tau^2} - \frac{\gamma t}{4}\right). \end{aligned} \quad (6.8)$$

For short times $\tau \ll 1$ one can show that the optimal squeezing angle is approximately given by

$$\vartheta_{\text{sq}} \simeq \frac{1}{2} \text{arccot} \left(\mathcal{I}_0\tau + \frac{\gamma}{4\chi} \right). \quad (6.9)$$

Note that in contradistinction with equation (4.12), for a given time τ the optimal squeezing angle is closer to 0 in the presence of dephasing. In a certain sense, dephasing makes the isocontour ellipsoid rotate faster (yet also making it smaller). Finally, the optimal squeezing amount turns out to be

$$\Delta^2 \hat{S}_\perp^{\text{opt}}(\vartheta, t) - |\langle \hat{S}_y(t) \rangle| \simeq 2\mathcal{I}_0^2\tau \left[\mathcal{I}_0\tau + \frac{\gamma}{4\chi} - \sqrt{1 + \left(\mathcal{I}_0\tau + \frac{\gamma}{4\chi} \right)^2} \right]. \quad (6.10)$$

In figure 5, we plot this optimal squeezing for several values of the ratio γ/χ . The degradation of this quantity with γ/χ can be clearly observed.

7. Concluding remarks

In summary, we have presented a quasiclassical approximation to the light propagation in a cross-Kerr medium. Even if the states considered are bright and we neglect quantum correlations, we still observe non-classical effects such as entanglement or squeezing. Interestingly, in the quasiclassical limit the correlations remain in the system once induced, as opposed to the periodical decorrelation observed in the exact evolution. We have also constructed a model for dephasing processes in these media, demonstrating that dissipation does visibly affect the degree of polarization, but not so much its vectorial direction.

Acknowledgments

Financial support from the EU FP7 (the grant Q-ESSENCE), the Spanish DGI (grant numbers FIS2008-04356 and FIS2011-26786), the UCM-BSCH program (grant number GR-920992) and the Mexican CONACyT (grant number 106525) is acknowledged.

Appendix A. The two-mode Wigner function

In this appendix a brief review of the Wigner distribution is given for the problem at hand. For a single mode a , the Wigner function for a state given by the density matrix $\hat{\rho}$ is defined as

$$W(\alpha) = \text{Tr}[\hat{\rho}_a \hat{w}(\alpha)], \quad (\text{A.1})$$

where the kernel $\hat{w}(\alpha)$ reads

$$\hat{w}(\alpha) = \frac{1}{\pi^2} \int d\lambda \exp(\alpha\lambda^* - \alpha^*\lambda) \hat{D}(\alpha), \quad (\text{A.2})$$

so it appears as the Fourier transform of the displacement operator $\hat{D}(\alpha)$, with

$$\hat{D}(\alpha) = \exp(\alpha\hat{a}^\dagger - \alpha^*\hat{a}). \quad (\text{A.3})$$

Note that the standard coherent states $|\alpha\rangle$ are generated by the action of $\hat{D}(\alpha)$ on the vacuum, i.e.

$$|\alpha\rangle = \hat{D}(\alpha)|0\rangle. \quad (\text{A.4})$$

For a coherent state $|\alpha_0\rangle$, the Wigner function is

$$W(\alpha) = \frac{2}{\pi} \exp(-2|\alpha - \alpha_0|). \quad (\text{A.5})$$

In a more general context, the Wigner function can be interpreted as the phase-space symbol of the density matrix $\hat{\rho}$. This notion can be extended to any operator \hat{O} in such a way that its symbol is given by

$$W_{\hat{O}}(\alpha) = \text{Tr}[\hat{O} \hat{w}(\alpha)]. \quad (\text{A.6})$$

In particular, for the basic mode operator \hat{a} we have

$$W_{\hat{a}} = \frac{\alpha}{\pi}. \quad (\text{A.7})$$

In terms of $W(\alpha)$, we can map any operator evolution into a differential equation using the following rules [105]:

$$\hat{a}\hat{\rho} \mapsto \left(\alpha + \frac{1}{2} \frac{\partial}{\partial \alpha^*}\right) W(\alpha), \quad \hat{a}^\dagger \hat{\rho} \mapsto \left(\alpha^* - \frac{1}{2} \frac{\partial}{\partial \alpha}\right) W(\alpha), \quad (\text{A.8})$$

$$\hat{\rho}\hat{a} \mapsto \left(\alpha - \frac{1}{2} \frac{\partial}{\partial \alpha^*}\right) W(\alpha), \quad \hat{\rho}\hat{a}^\dagger \mapsto \left(\alpha^* + \frac{1}{2} \frac{\partial}{\partial \alpha}\right) W(\alpha),$$

and after performing the decomposition (2.6), this reads

$$\delta\hat{a}\hat{\rho} \mapsto \frac{1}{2} \frac{\partial}{\partial \alpha^*} W, \quad \delta\hat{a}^\dagger \hat{\rho} \mapsto -\frac{1}{2} \frac{\partial}{\partial \alpha} W, \quad (\text{A.9})$$

$$\hat{\rho}\delta\hat{a} \mapsto -\frac{1}{2} \frac{\partial}{\partial \alpha^*} W, \quad \hat{\rho}\delta\hat{a}^\dagger \mapsto \frac{1}{2} \frac{\partial}{\partial \alpha} W$$

and analogous ones for the b mode.

The two-mode Wigner function is given by a direct generalization of equation (A.1), namely

$$W(\alpha, \beta) = \text{Tr}[\hat{\rho} \hat{w}(\alpha) \hat{w}(\beta)]. \quad (\text{A.10})$$

The rest of the properties needed in the paper can be extended to this two-mode case in a direct way.

Appendix B. Purity of the reduced density matrix

For completeness, we give here some intermediate steps to obtain the expression (3.6) for the reduced purity $P_a(\tau)$, which is defined as

$$P_a(\tau) = \frac{\pi}{8} \int_{-\pi}^{\pi} d\varphi_a \int_0^\infty d\mathcal{J}_a \left[\int_{-\pi}^{\pi} d\varphi_b \int_0^\infty d\mathcal{J}_b W(\mathcal{J}_a, \varphi_a; \mathcal{J}_b, \varphi_b | \tau) \right]^2. \quad (\text{B.1})$$

Employing the form of the explicit form of the Wigner function (2.11) we have

$$\begin{aligned} P_a(\tau) &= \frac{2}{\pi^3} \int_{-\pi}^{\pi} d\varphi_a d\varphi_1 d\varphi_2 \int_0^\infty d\mathcal{J}_a d\mathcal{J}_1 d\mathcal{J}_2 \exp(-4\mathcal{J}_a - 4\mathcal{J}_{0a} - 2\mathcal{J}_1 - 2\mathcal{J}_2 - 4\mathcal{J}_{0b}) \\ &\quad \times \exp \left[2\sqrt{\mathcal{J}_a \mathcal{J}_{0a}} (e^{i\varphi_a + 2i\mathcal{J}_1\tau} + e^{i\varphi_a + 2i\mathcal{J}_2\tau} + e^{-i\varphi_a - 2i\mathcal{J}_1\tau} + e^{-i\varphi_a - 2i\mathcal{J}_2\tau}) \right] \\ &\quad \times \exp(4\sqrt{\mathcal{J}_1 \mathcal{J}_{0b}} \cos \varphi_1 + 4\sqrt{\mathcal{J}_2 \mathcal{J}_{0b}} \cos \varphi_2). \end{aligned} \quad (\text{B.2})$$

In the second line, we can expand the exponential in power series in $e^{i\varphi_a}$ and $e^{-i\varphi_a}$, considering the rest of the variables as fixed coefficients. Then, the integration over φ_a can be explicitly carried out, with the result

$$2\pi \sum_{k=0}^{\infty} \frac{(4\mathcal{J}_a)^k (2\mathcal{J}_{0a})^k}{(k!)^2} \{1 + \cos [2(\mathcal{J}_1 - \mathcal{J}_2)\tau]\}^k. \quad (\text{B.3})$$

Together with the term $e^{-4\mathcal{J}_a}$, this can be immediately integrated over $d\mathcal{J}_a$, yielding

$$\frac{\pi}{4} \exp \{2\mathcal{J}_{0a} [1 + \cos (2(\mathcal{J}_1 - \mathcal{J}_2)\tau)]\}, \quad (\text{B.4})$$

which replaces the second line in equation (B.2). The integrations over φ_j transform the last line of (B.2) into

$$(2\pi)^2 I_0(4\sqrt{\mathcal{I}_1 \mathcal{I}_{0b}}) I_0(4\sqrt{\mathcal{I}_2 \mathcal{I}_{0b}}). \quad (\text{B.5})$$

Finally, to carry out the integrations over \mathcal{I}_1 and \mathcal{I}_2 , we expand the Bessel functions in power series, namely

$$I_0(4\sqrt{\mathcal{I}_j \mathcal{I}_{0b}}) = \sum_{k=0}^{\infty} \frac{(2\mathcal{I}_j)^k (2\mathcal{I}_{0b})^k}{(k!)^2}, \quad (\text{B.6})$$

as well as the exponential in (B.4)

$$\exp[2\mathcal{I}_{0a} \cos(2(\mathcal{I}_1 - \mathcal{I}_2)\tau)] = \sum_{n=-\infty}^{\infty} I_n(2\mathcal{I}_{0a}) \exp[2i(\mathcal{I}_1 - \mathcal{I}_2)\tau]. \quad (\text{B.7})$$

All this enables a direct integration over \mathcal{I}_1 and \mathcal{I}_2 , yielding

$$P(\tau) = 4 \exp(-4\mathcal{I}_{0b} - 2\mathcal{I}_{0a}) \int_0^{\infty} d\mathcal{I}_1 d\mathcal{I}_2 \exp(-2\mathcal{I}_1 - 2\mathcal{I}_2) \\ \times \sum_{k,m=0}^{\infty} \frac{(2\mathcal{I}_1)^k (2\mathcal{I}_2)^m (2\mathcal{I}_{0b})^{k+m}}{(k!)^2 (m!)^2} \sum_{n=-\infty}^{\infty} I_n(2\mathcal{I}_{0a}) e^{2i(\mathcal{I}_1 - \mathcal{I}_2)\tau}. \quad (\text{B.8})$$

From this expression, the result (3.6) for the purity follows straightforwardly.

References

- [1] Braginsky V B 1968 *Sov. Phys.—JETP* **26** 831–4
- [2] Unruh W G 1979 *Phys. Rev. D* **19** 2888–96
- [3] Milburn G J and Walls D F 1983 *Phys. Rev. A* **28** 2065–70
- [4] Imoto N, Haus H A and Yamamoto Y 1985 *Phys. Rev. A* **32** 2287–92
- [5] Alsing P, Milburn G J and Walls D F 1988 *Phys. Rev. A* **37** 2970–8
- [6] Grangier P, Levenson J A and Poizat J P 1998 *Nature* **396** 537–42
- [7] Sanders B C and Milburn G J 1989 *Phys. Rev. A* **39** 694–702
- [8] König F, Büchler B, Rechtenwald T, Leuchs G and Sizmman A 2002 *Phys. Rev. A* **66** 043810
- [9] Xiao Y F, Özdemir S K, Gaddam V, Dong C H, Imoto N and Yang L 2008 *Opt. Express* **16** 21462–75
- [10] Milburn G J and Holmes C A 1986 *Phys. Rev. Lett.* **56** 2237–40
- [11] Yurke B and Stoler D 1986 *Phys. Rev. Lett.* **57** 13–6
- [12] Tombesi P and Mecozzi A 1987 *J. Opt. Soc. Am. B* **4** 1700–9
- [13] Gantsog T and Tanaš R 1991 *J. Mod. Opt.* **38** 1537–58
- [14] Wilson-Gordon A D, Bužek V and Knight P L 1991 *Phys. Rev. A* **44** 7647–56
- [15] Tara K, Agarwal G S and Chaturvedi S 1993 *Phys. Rev. A* **47** 5024–9
- [16] Luis A, Sánchez-Soto L L and Tanaš R 1995 *Phys. Rev. A* **51** 1634–43
- [17] Szabo S, Adam P, Janszky J and Domokos P 1996 *Phys. Rev. A* **53** 2698–710
- [18] Chumakov S M, Frank A and Wolf K B 1999 *Phys. Rev. A* **60** 1817–23
- [19] Korolkova N, Loudon R, Gardavsky G, Hamilton M W and Leuchs G 2001 *J. Mod. Opt.* **48** 1339–55
- [20] Vitali D, Fortunato M and Tombesi P 2000 *Phys. Rev. Lett.* **85** 445–8
- [21] Jian Z, Ming Y, Yan L and Zhuo-Liang C 2009 *Chin. Phys. Lett.* **26** 100301
- [22] Zhu M, Yin X and Yuan G 2011 *Opt. Commun.* **284** 3483–7
- [23] Turchette Q A, Hood C J, Lange W, Mabuchi H and Kimble H J 1995 *Phys. Rev. Lett.* **75** 4710–3

- [24] Semião F L and Vidiella-Barranco A 2005 *Phys. Rev. A* **72** 064305
- [25] Matsuda N, Mitsumori Y, Kosaka H, Edamatsu K and Shimizu R 2007 *Appl. Phys. Lett.* **91** 171119
- [26] Azuma H 2008 *J. Phys. D: Appl. Phys.* **41** 025102
- [27] You H and Franson J 2012 *Quantum Inf. Process.* **11** 1627–51
- [28] Xia Y, Song J, Lu P M and Song H S 2011 *J. Phys. B: At. Mol. Opt. Phys.* **44** 025503
- [29] Kok P, Lee H and Dowling J P 2002 *Phys. Rev. A* **66** 063814
- [30] Munro W J, Nemoto K, Beausoleil R G and Spiller T P 2005 *Phys. Rev. A* **71** 033819
- [31] Greentree A D, Beausoleil R G, Hollenberg L C L, Munro W J, Nemoto K, Prawer S and Spiller T P 2009 *New J. Phys.* **11** 093005
- [32] Schmidt H and Imamoğlu A 1996 *Opt. Lett.* **21** 1936–8
- [33] Imamoğlu A, Schmidt H, Woods G and Deutsch M 1997 *Phys. Rev. Lett.* **79** 1467–70
- [34] Werner M J and Imamoğlu A 1999 *Phys. Rev. A* **61** 011801
- [35] Dey T N and Agarwal G S 2007 *Phys. Rev. A* **76** 015802
- [36] Hau L, Harris S, Dutton Z and Behroozi C 1999 *Nature* **397** 594–8
- [37] Kang H and Zhu Y 2003 *Phys. Rev. Lett.* **91** 093601
- [38] Castellanos-Beltran M A and Lehnert K W 2007 *Appl. Phys. Lett.* **91** 083509
- [39] Mallet F, Ong F R, Palacios-Laloy A, Nguyen F, Bertet P, Vion D and Esteve D 2009 *Nature Phys.* **5** 791–5
- [40] Bergeal N, Schackert F, Metcalfe M, Vijay R, Manucharyan V E, Frunzio L, Prober D E, Schoelkopf R J, Girvin S M and Devoret M H 2010 *Nature* **465** 64–8
- [41] Bermel P, Rodriguez A, Joannopoulos J D and Soljačić M 2007 *Phys. Rev. Lett.* **99** 053601
- [42] Mohapatra A K, Bason M G, Butscher B, Weatherill K J and Adams C S 2008 *Nature Phys.* **4** 890–4
- [43] Brandão F G S L, Hartmann M J and Plenio M B 2008 *New J. Phys.* **10** 043010
- [44] Babourina-Brooks E, Doherty A and Milburn G J 2008 *New J. Phys.* **10** 105020
- [45] Ritze H H and Bandilla A 1979 *Opt. Commun.* **29** 126–30
- [46] Heiman D, Hellwarth R W, Levenson M D and Martin G 1976 *Phys. Rev. Lett.* **36** 189–92
- [47] Yuen H P and Shapiro J H 1979 *Opt. Lett.* **4** 334–6
- [48] Levenson M D, Shelby R M and Perlmutter S H 1985 *Opt. Lett.* **10** 514–6
- [49] Levenson M D, Shelby R M, Aspect A, Reid M and Walls D F 1985 *Phys. Rev. A* **32** 1550–62
- [50] Kitagawa M and Yamamoto Y 1986 *Phys. Rev. A* **34** 3974–88
- [51] Joneckis L G and Shapiro J H 1993 *J. Opt. Soc. Am. B* **10** 1102–20
- [52] Sundar K 1996 *Phys. Rev. A* **53** 1096–111
- [53] Schmitt S, Ficker J, Wolff M, König F, Sizmann A and Leuchs G 1998 *Phys. Rev. Lett.* **81** 2446–9
- [54] Boyd R W 1999 *J. Mod. Opt.* **46** 367–78
- [55] Shelby R M, Levenson M D and Bayer P W 1985 *Phys. Rev. B* **31** 5244–52
- [56] Elser D, Andersen U L, Korn A, Glöckl O, Lorenz S, Marquardt C and Leuchs G 2006 *Phys. Rev. Lett.* **97** 133901
- [57] Agrawal G P 2007 *Nonlinear Fiber Optics* 4th edn (New York: Academic)
- [58] Lee H W 1995 *Phys. Rep.* **259** 147–211
- [59] Schroek F E 1996 *Quantum Mechanics on Phase Space* (Dordrecht: Kluwer)
- [60] Schleich W P 2001 *Quantum Optics in Phase Space* (Berlin: Wiley-VCH)
- [61] Heller E J 1976 *J. Chem. Phys.* **65** 1289–98
- [62] Lee H W and Scully M O 1980 *J. Chem. Phys.* **73** 2238–42
- [63] Balzer B, Dilthey S, Stock G and Thos M 2003 *J. Chem. Phys.* **119** 5795–804
- [64] Hillery M, O’Connell R F, Scully M O and Wigner E P 1984 *Phys. Rep.* **106** 121–67
- [65] Drobný G, Bandilla A and Jex I 1997 *Phys. Rev. A* **55** 78–93
- [66] Banaszek K and Knight P L 1997 *Phys. Rev. A* **55** 2368–75
- [67] Bandilla A, Drobný G and Jex I 2000 *J. Opt. B: Quantum Semiclass. Opt.* **2** 265–70
- [68] Stobińska M, Milburn G J and Wódkiewicz K 2008 *Phys. Rev. A* **78** 013810
- [69] Corney J F, Heersink J, Dong R, Josse V, Drummond P D, Leuchs G and Andersen U L 2008 *Phys. Rev. A* **78** 023831

- [70] Sizmman A and Leuchs G 1999 The optical Kerr effect and quantum optics in fibers *Progress in Optics* vol 39 ed E Wolf (Amsterdam: Elsevier) pp 373–469
- [71] Duan L M, Giedke G, Cirac J I and Zoller P 2000 *Phys. Rev. Lett.* **84** 2722–5
- [72] Simon R 2000 *Phys. Rev. Lett.* **84** 2726–9
- [73] Weiss U 1999 *Quantum Dissipative Systems* (Singapore: World Scientific)
- [74] Scully M O and Zubairy M S 2001 *Quantum Optics* (Cambridge: Cambridge University Press)
- [75] Goldstein H 1980 *Classical Mechanics* (New York: Addison-Wesley)
- [76] Heersink J, Gaber T, Lorenz S, Glöckl O, Korolkova N and Leuchs G 2003 *Phys. Rev. A* **68** 013815
- [77] Heersink J, Josse V, Leuchs G and Andersen U L 2005 *Opt. Lett.* **30** 1192–4
- [78] Braunstein S L and van Loock P 2005 *Rev. Mod. Phys.* **77** 513–77
- [79] Ferraro A, Olivares S and Paris M G A 2005 *Gaussian States in Quantum Information* (Naples: Bibliopolis)
- [80] Wanga X B, Hiroshima T, Tomita A and Hayashi M 2007 *Phys. Rep.* **448** 1–111
- [81] Adesso G and Illuminati F 2007 *J. Phys. A: Math. Theor.* **40** 7821–80
- [82] Weedbrook C, Pirandola S, García-Patrón R, Cerf N J, Ralph T C, Shapiro J H and Lloyd S 2012 *Rev. Mod. Phys.* **84** 621–69
- [83] Shchukin E and Vogel W 2005 *Phys. Rev. Lett.* **95** 230502
- [84] Agarwal G S and Biswas A 2005 *New J. Phys.* **7** 211
- [85] Hillery M and Zubairy M S 2006 *Phys. Rev. Lett.* **96** 050503
- [86] Gomes R M, Salles A, Toscano F, Souto Ribeiro P H and Walborn S P 2009 *Proc. Natl Acad. Sci. USA* **106** 21517–20
- [87] Mazzola L, Bellomo B, Lo Franco R and Compagno G 2010 *Phys. Rev. A* **81** 052116
- [88] De Pasquale A, Facchi P, Parisi G, Pascazio S and Scardicchio A 2010 *Phys. Rev. A* **81** 052324
- [89] Pasquale A D, Facchi P, Giovannetti V, Parisi G, Pascazio S and Scardicchio A 2012 *J. Phys. A: Math. Theor.* **45** 015308
- [90] Abramowitz M and Stegun I A (ed) 1984 *Handbook of Mathematical Functions* (New York: Dover)
- [91] Luis A and Sánchez-Soto L L 2000 Quantum phase difference, phase measurements and Stokes operators *Progress in Optics* vol 41 ed E Wolf (Amsterdam: Elsevier) pp 421–81
- [92] Sehat A, Söderholm J, Björk G, Espinoza P, Klimov A B and Sánchez-Soto L L 2005 *Phys. Rev. A* **71** 033818
- [93] Marquardt C, Heersink J, Dong R, Chekhova M V, Klimov A B, Sánchez-Soto L L, Andersen U L and Leuchs G 2007 *Phys. Rev. Lett.* **99** 220401
- [94] Björk G, Söderholm J, Sánchez-Soto L L, Klimov A B, Ghiu I, Marian P and Marian T A 2010 *Opt. Commun.* **283** 4440–7
- [95] Müller C R, Stoklasa B, Peuntinger C, Gabriel C, Řeháček J, Hradil Z, Klimov A B, Leuchs G, Marquardt C and Sánchez-Soto L L 2012 *New J. Phys.* **14** 085002
- [96] Chirkin A S, Orlov A A and Parashchuk D Y 1993 *Quantum Electron.* **23** 870–4
- [97] Korolkova N, Leuchs G, Loudon R, Ralph T C and Silberhorn C 2002 *Phys. Rev. A* **65** 052306
- [98] Luis A and Korolkova N 2006 *Phys. Rev. A* **74** 043817
- [99] Mahler D, Joanis P, Vilim R and de Guise H 2010 *New J. Phys.* **12** 033037
- [100] Ma J, Wang X, Sun C P and Nori F 2011 *Phys. Rep.* **509** 89–165
- [101] Klimov A B, Delgado J and Sánchez-Soto L L 2006 *Opt. Commun.* **258** 210–8
- [102] Zurek W H 2003 *Rev. Mod. Phys.* **75** 715–75
- [103] Shao J, Ge M L and Cheng H 1996 *Phys. Rev. E* **53** 1243–5
- [104] Mozyrsky D and Privman V 1998 *J. Stat. Phys.* **91** 787–99
- [105] Gardiner C W and Zoller P 2004 *Quantum Noise* 2nd edn (Berlin: Springer)
- [106] Breuer H P and Petruccione F 2002 *The Theory of Open Quantum Systems* (Oxford: Oxford University Press)
- [107] Klimov A B, Romero J L, Sánchez-Soto L L, Messina A and Napoli A 2008 *Phys. Rev. A* **77** 033853